

# 轴向均布荷载下弯剪型竖向悬臂杆的屈曲临界荷载简化算法

李亮<sup>1</sup>, 李国强<sup>2</sup>

(1. 长安大学建筑工程学院, 陕西 西安 710061;  
2. 同济大学土木工程防灾国家重点实验室, 上海 200092)

**摘要:**根据竖向悬臂杆的边界条件、弯曲及剪切屈曲侧移曲线,选取了含有三角函数的表达式来近似表示竖向悬臂杆的弯曲分量和剪切分量,然后利用能量法推导了在轴向均布荷载作用下弯剪型悬臂杆的屈曲临界荷载简化计算公式。通过与有限元计算结果对比,验证了简化算法的可靠性。最后,将本文提出的竖向均布荷载作用下临界荷载计算公式与 Timoshenko 提出的顶点集中荷载下临界荷载经典理论公式进行对比,发现本文提出的临界荷载计算公式多了一个无量纲的系数,通过参数分析,研究了该系数对公式计算精度的影响。

**关键词:**竖向悬臂杆; 边界条件; 三角函数; 弯曲分量; 屈曲临界荷载

中图分类号: TU 375.4

文献标志码: A

文章编号: 1006-7930(2013)06-0817-05

结构屈曲是指在外荷载作用下结构的平衡状态开始丧失,稍有扰动变形便迅速增大,最后使结构破坏<sup>[1-4]</sup>。对于竖向悬臂杆的屈曲问题的研究表明:对于以弯曲变形为主的竖向悬臂杆,忽略剪切变形往往并不会造成较大误差<sup>[4-6]</sup>;对于剪切变形影响较大的竖向悬臂杆,则必须考虑剪切变形的影响<sup>[6-7]</sup>。

Timoshenko 和 Gere(1961)<sup>[1]</sup>提出了在顶点集中荷载作用下,弯剪型竖向悬臂杆的屈曲临界荷载:

$$P_{cr} = \frac{P_{cr,D}}{1 + P_{cr,D}/P_{cr,S}} \quad (1)$$

式中:  $P_{cr,D}$ 、 $P_{cr,S}$  分别为弯曲和剪切屈曲临界荷载。

但工程中竖向悬臂杆结构,如高层建筑,所受的荷载并非顶点集中荷载,多为轴向均布荷载。Timoshenko<sup>[1]</sup>根据能量法推导了弯曲型悬臂杆在轴向均布荷载作用下屈曲临界荷载的计算公式,由于该算法仅考虑了结构的弯曲变形,当计算可忽略剪切变形悬臂杆件临界荷载时具有良好的精度。

Timoshenko 曾指出,在均布荷载作用下竖向悬臂杆的轴力是变化的,其屈曲时侧移曲线的微分方程为变系数方程,难以得到解析解。于是, Bakker<sup>[3]</sup>根据能量法提出了在均布荷载作用下竖向悬臂柱的弯剪型屈曲临界荷载计算公式,假设剪切型屈曲模态为:当  $0 \leq x \leq h$  时,  $y = (x/h)y_{top}$ ; 当  $h \leq x \leq L$  时,  $y = y_{top}$ , 如图 1 所示。由于纯剪切屈曲模态与真实的屈曲模态存在较大差异,因此该算法计算结果存在较大误差。

本文利用能量法推导在竖向均布荷载作用下弯剪型悬臂杆的屈曲临界荷载简化计算公式,从理论上研究竖向均布荷载作用下的弯剪型竖向悬臂杆的临界荷载计算公式也存在类

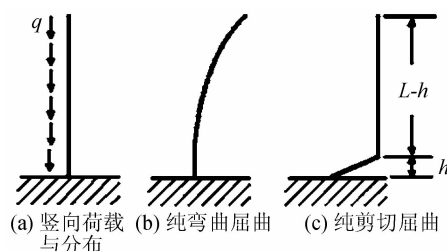


图 1 竖向悬臂杆在均布荷载作用下的屈曲模态

Fig. 1 Buckling Mode of the Vertical Cantilever Bar under Uniformly Distributed Load

似于顶点集中荷载作用下式(1)的临界荷载的表达式,只不过公式中增加了一个参数 $\eta$ .采用有限元方法验证了简化算法的可靠性,并给出可忽略参数 $\eta$ 时,参数 $\rho$ 的适用范围.

## 1 弯剪型悬臂竖杆屈曲承载力简化算法

### 1.1 纯弯曲及纯剪切临界荷载

竖向悬臂杆的纯弯曲屈曲变形近似于余弦曲线,而纯剪切屈曲变形近似于正弦曲线,故假定纯弯曲侧移 $y_b$ 和纯剪切侧移 $y_s$ <sup>[1,7-9]</sup>:

$$y_b = A(1 - \cos \frac{\pi x}{2L}) \quad (2)$$

$$y_s = B \sin \frac{\pi x}{2L} \quad (3)$$

式中: $A$ 、 $B$ 分别为竖向悬臂杆发生纯弯曲变形和纯剪切变形的最大值,为公式的待定常系数.

纯弯曲总势能:

$$\Pi_b = U_b + V_b = \int_0^L \frac{M^2}{2D} dx - \frac{q}{2} \int_0^L (L-x) \left( \frac{dy}{dx} \right)^2 dx = \frac{D}{2} \left( \frac{\pi}{2L} \right)^4 \frac{L}{2} A^2 - \frac{q}{2} \left( \frac{\pi}{2L} \right)^2 L^2 \left( \frac{1}{4} - \frac{1}{\pi^2} \right) A^2 \quad (4)$$

式中: $D$ 为结构的弯曲刚度; $L$ 为结构的总高度; $q$ 为作用在结构上的竖向均布荷载; $M$ 为当结构发生侧移时竖向均布荷载 $q$ 在 $x$ 高度处产生的弯矩.

纯剪切总势能:

$$\Pi_s = U_s + V_s = \int_0^L \frac{Q^2}{2C} dx - \frac{q}{2} \int_0^L (L-x) \left( \frac{dy}{dx} \right)^2 dx = \frac{C}{2} \left( \frac{\pi}{2L} \right)^2 \frac{L}{2} B^2 - \frac{q}{2} \left( \frac{\pi}{2L} \right)^2 \left( \frac{1}{4} + \frac{1}{\pi^2} \right) L^2 B^2 \quad (5)$$

式中: $C$ 为结构的弯曲刚度; $Q$ 为当结构发生侧移时竖向均布荷载 $q$ 在 $x$ 高度处产生的剪力.

由势能驻值条件,可得到纯弯曲和纯剪切的屈曲临界荷载:

$$q_{cr,b} = \frac{\pi^4 D}{2(\pi^2 - 4)L^3} \quad (6)$$

$$q_{cr,s} = \frac{2\pi^2 C}{(\pi^2 + 4)L} \quad (7)$$

### 1.2 弯剪型悬臂竖杆屈曲荷载

当结构发生弯剪屈曲时,结构的变形分为由弯矩引起的变形 $y_b$ 和由剪力产生的变形 $y_s$ ,总变形为两者之和,即:

$$y = y_b + y_s \quad (8)$$

结构总的应变势能:

$$U = U_b + U_s = \frac{D}{2} A^2 \left( \frac{\pi}{2L} \right)^4 \frac{L}{2} + \frac{C}{2} B^2 \left( \frac{\pi}{2L} \right)^2 \frac{L}{2} \quad (9)$$

竖向均布荷载势能:

$$\begin{aligned} V &= -\frac{q}{2} \int_0^L (L-x) \left( \frac{dy_b}{dx} + \frac{dy_s}{dx} \right)^2 dx \\ &= -\frac{q}{2} \left( \frac{\pi}{2L} \right)^2 \int_0^L \left( L \left( A^2 \sin^2 \frac{\pi x}{2L} + 2AB \sin \frac{\pi x}{2L} \cos \frac{\pi x}{2L} + B^2 \cos^2 \frac{\pi x}{2L} \right) \right. \\ &\quad \left. - x \left( A^2 \sin^2 \frac{\pi x}{2L} + 2AB \sin \frac{\pi x}{2L} \cos \frac{\pi x}{2L} + B^2 \cos^2 \frac{\pi x}{2L} \right) \right) dx \end{aligned} \quad (10)$$

式中

$$A^2 \int_0^L \sin^2 \frac{\pi x}{2L} dx = A^2 \int_0^L \frac{1 - \cos \frac{\pi x}{L}}{2} dx = \frac{L}{2} A^2 \quad (11)$$

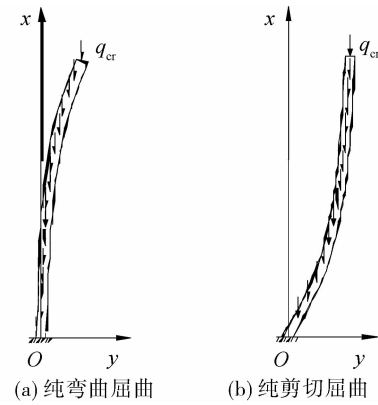


图2 两类竖向荷载作用下悬臂柱的屈曲

Fig. 2 Two types of Buckling of the Vertical Cantilever Bar under Uniformly Distributed Load

$$2AB \int_0^L \sin \frac{\pi x}{2L} \cos \frac{\pi x}{2L} dx = AB \int_0^L \sin \frac{\pi x}{L} dx = AB \frac{2L}{\pi} \quad (12)$$

$$B^2 \int_0^L \cos^2 \frac{\pi x}{2L} dx = B^2 \int_0^L \frac{1 + \cos \frac{\pi x}{L}}{2} dx = B^2 \frac{L}{2} \quad (13)$$

$$A^2 \int_0^L x \sin^2 \frac{\pi x}{2L} dx = A^2 \int_0^L x \frac{1 - \cos \frac{\pi x}{L}}{2} dx = \frac{A^2}{2} \left[ \frac{L^2}{2} + 2 \left( \frac{L}{\pi} \right)^2 \right] \quad (14)$$

$$2AB \int_0^L x \sin \frac{\pi x}{2L} \cos \frac{\pi x}{2L} dx = AB \int_0^L x \sin \frac{\pi x}{L} dx = \frac{L^2}{\pi} AB \quad (15)$$

$$B^2 \int_0^L x \cos^2 \frac{\pi x}{2L} dx = B^2 \int_0^L x \frac{1 + \cos \frac{\pi x}{L}}{2} dx = \frac{B^2}{2} \left[ \frac{L^2}{2} - 2 \left( \frac{L}{\pi} \right)^2 \right] \quad (16)$$

整理后,可得到:

$$V = -\frac{q}{2} \left( \frac{\pi}{2L} \right)^2 L^2 \left[ A^2 \left( \frac{1}{4} - \frac{1}{\pi^2} \right) + AB \frac{1}{\pi} + B^2 \left( \frac{1}{4} + \frac{1}{\pi^2} \right) \right] \quad (17)$$

结构的总势能:

$$\begin{aligned} \Pi = U + V &= \frac{D}{2} A^2 \left( \frac{\pi}{2L} \right)^4 \frac{L}{2} + \frac{C}{2} B^2 \left( \frac{\pi}{2L} \right)^2 \frac{L}{2} \\ &\quad - \frac{q}{2} \left( \frac{\pi}{2L} \right)^2 L^2 \left[ A^2 \left( \frac{1}{4} - \frac{1}{\pi^2} \right) + AB \frac{1}{\pi} + B^2 \left( \frac{1}{4} + \frac{1}{\pi^2} \right) \right] \end{aligned} \quad (18)$$

由势能驻值条件,对上式进行变分有:

$$\frac{\partial \Pi}{\partial A} = \frac{1}{2} \left( \frac{\pi}{2L} \right)^2 L \left\{ \left[ D \left( \frac{\pi}{2L} \right)^2 - qL \left( \frac{1}{2} - \frac{2}{\pi^2} \right) \right] A - q \frac{L}{\pi} B \right\} = 0 \quad (19)$$

$$\frac{\partial \Pi}{\partial B} = \frac{1}{2} \left( \frac{\pi}{2L} \right)^2 L \left\{ -q \frac{L}{\pi} A + \left[ C - qL \left( \frac{1}{2} + \frac{2}{\pi^2} \right) \right] B \right\} = 0 \quad (20)$$

由于  $A, B$  有非零解的条件是系数行列式为零,即

$$\left| D \left( \frac{\pi}{2L} \right)^2 - qL \left( \frac{1}{2} - \frac{2}{\pi^2} \right) - q \frac{L}{\pi} - q \frac{L}{\pi} C - qL \left( \frac{1}{2} + \frac{2}{\pi^2} \right) \right| = 0 \quad (21)$$

由上式可得,结构发生弯剪屈曲时的临界荷载方程为:

$$(qL)^2 \left[ \left( \frac{1}{2} + \frac{2}{\pi^2} \right) \left( \frac{1}{2} - \frac{2}{\pi^2} \right) - \frac{1}{\pi^2} \right] - (qL) \left[ D \left( \frac{\pi}{2L} \right)^2 \left( \frac{1}{2} + \frac{2}{\pi^2} \right) + C \left( \frac{1}{2} - \frac{2}{\pi^2} \right) \right] + DC \left( \frac{\pi}{2L} \right)^2 = 0 \quad (22)$$

解方程得到:

$$q_{cr} = \frac{\left[ \frac{1}{8} \frac{D}{L^2} (\pi^2 + 4) + \frac{1}{2\pi^2} C(\pi^2 - 4) \right] \pm \sqrt{\left[ \frac{1}{8} \frac{D}{L^2} (\pi^2 + 4) + \frac{1}{2\pi^2} C(\pi^2 - 4) \right]^2 + DC \frac{1}{L^2}}}{\frac{2}{\pi^2} \left[ \frac{1}{4\pi^2} (\pi^2 + 4)(\pi^2 - 4) - 1 \right] L} \quad (23)$$

令  $\rho = \sqrt{\frac{CL^2}{D}}$ , 则  $\rho$  是无量纲的参数, 具有长细比的特性.

再令  $\mu = \frac{1}{\rho^2} \left( \frac{\pi}{2} \right)^2 = \frac{D}{CL^2} \left( \frac{\pi}{2} \right)^2$ , 则式(23)可整理为:

$$\begin{aligned} q_{cr} &= \frac{\left[ [\mu(\pi^2 + 4) + (\pi^2 - 4)] - \sqrt{[\mu(\pi^2 + 4) - (\pi^2 - 4)]^2 + 16\mu\pi^2} \right] [\mu(\pi^2 + 4) + (\pi^2 - 4)]}{[2\mu[(\pi^2 + 4)(\pi^2 - 4) - 4\pi^2]]} \\ &\quad \times \left( \frac{\pi^4 D}{2(\pi^2 - 4)L^3} \right) / \left\{ 1 + \frac{\pi^4 D / [2(\pi^2 - 4)L^3]}{2\pi^2 D / [(\pi^2 + 4)L]} \right\} \end{aligned} \quad (24)$$

再令

$$\eta = \frac{\left[ [\mu(\pi^2 + 4) + (\pi^2 - 4)] - \sqrt{[\mu(\pi^2 + 4) - (\pi^2 - 4)]^2 + 16\mu\pi^2} \right] [\mu(\pi^2 + 4) + (\pi^2 - 4)]}{2\mu[(\pi^2 + 4)(\pi^2 - 4) - 4\pi^2]} \quad (25)$$

显然,参数  $\eta$  仅与  $\mu$  有关.

且已知  $q_{cr,s} = \frac{2\pi^2 C}{(\pi^2 + 4)L}$ ,  $q_{cr,b} = \frac{\pi^4 D}{2(\pi^2 - 4)L^3}$

于是,弯剪型屈曲的临界荷载为:

$$q_{cr} = \eta \frac{q_{cr,b}}{1 + \frac{q_{cr,b}}{q_{cr,s}}} \quad (26)$$

## 2 有限元方法对比

本文采用有限元软件 SAP2000 对本文提出临界荷载计算公式的可靠性进行验证. 模型单元采用杆系梁柱单元,该单元能够模拟杆件的弯曲变形和剪切变形. 模型为底部固接的竖向悬臂杆.

为了证明无论是对于以弯曲变形为主的杆件,还是剪切变形为主的杆件,本文提出的临界荷载计算公式均具有良好的精度,通过改变杆件弯曲刚度和剪切刚度之间的相对强弱程度得到了 6 个计算模型. 通过对计算模型进行屈曲分析,并将式(26)计算得到的屈曲承载力与有限元分析得到的屈曲承载力进行比较,以验证式(26)的可靠性.

算例介绍:模型总高度均为  $H = 14$  m,钢材均选取 Q235. 为了增大剪切变形的影响,各模型剪切刚度  $C$  均取原剪切刚度的 20%. 观察发现,所有模型的屈曲模态均表现为有侧移失稳. 将式(26)的计算结果与有限元分析结果对比可知,误差仅为 5%~8%,如表 1 所示. 与复杂的有限元方法相比,式(26)不仅应用简便,而且具有较好的精度.

## 3 参数 $\rho$ 对 $\eta$ 的影响

式(26)与式(1)形式非常相似,只是式(26)多出一个系数  $\eta$ . 那么,忽略参数  $\eta$  是否会对计算结果产生较大影响? 下面本文将对参数  $\eta$  的变化范围进行研究,并探讨在工程设计中忽略参数  $\eta$  对计算结果的影响.

根据式(25),可得到参数  $\eta$  随参数  $\rho$  的变化情况,如图 3 所示. 观察可知:

(1)当参数  $\rho < 2.5$  时,参数  $\eta$  随着  $\rho$  的增大而逐渐增大,且增大速度逐渐减慢;当  $\rho = 2.5$  时,可得到  $\eta_{max} = 1.179$ .

(2)当参数  $\rho > 2.5$  时时,参数  $\eta$  随着  $\rho$  的增大而逐渐减小,且随着  $\lambda$  的增大,减小的速度逐渐降低.

(3)对于任意  $\rho$ ,参数  $\eta$  始终大于 1. 因此,在工程设计中忽略参数  $\eta$  的影响会导致计算结果略低,在工程设计中是偏于安全的.

表 1 理论公式与有限元分析得到的屈曲承载力对比

Tab. 1 Comparison of the Buckling Capacity by Theoretical Formula and FEM

编 号	截面	抗弯刚度 $D$ $/N \cdot mm^{-1}$	抗剪刚度 $C$ $/N$	$\lambda$	$q_{cr}$ 公式 (26)	FEM	误差 /%
1	H150×100×8×10	2.26E+12	4.68E+07	64	6.82	6.43	5.70
2	H200×120×8×10	5.11E+12	5.91E+07	48	15.44	14.55	5.80
3	H300×150×10×12	1.84E+13	9.78E+07	32	55.62	52.28	6.01
4	H400×200×10×12	4.50E+13	1.32E+08	24	135.41	126.77	6.38
5	H500×200×10×12	7.51E+13	1.47E+08	20	225.55	210.70	6.58
6	H600×300×10×12	1.56E+14	1.99E+08	16	467.40	432.54	7.46

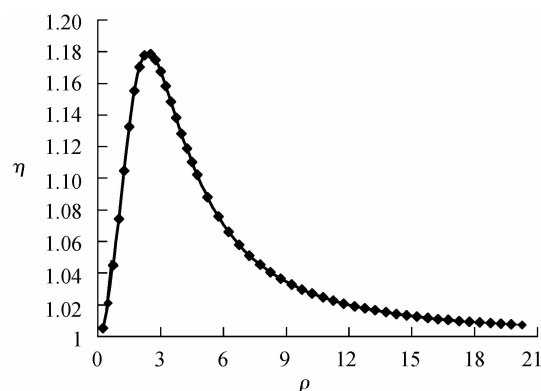


图 3 参数  $\eta$ - $\rho$  的关系曲线

Fig. 3 Relation Curve of the Parameter  $\eta$  and  $\rho$

(4)当 $0.79 < \rho < 7.35$ 时,参数 $\eta$ 始终大于1.05,此时忽略参数 $\eta$ 将导致误差超过5%,如表2所示。

表2列出了参数 $\rho$ 与参数 $\eta$ 的相互关系。在工程实际中,当已知结构的参数 $\rho$ 后,也可以根据工程精度的要求,通过查询表2来判断在运用式(26)计算结构屈曲承载力时,是否可以忽略参数 $\eta$ 。

## 4 结论

本文利用能量法推导了在竖向均布荷载作用下弯剪型悬臂杆的屈曲临界荷载简化计算公式,得到以下结论:

(1)通过与有限元计算结果对比,证明了提出的弯剪型悬臂杆在竖向均布荷载作用下的屈曲临界荷载计算公式能够较为准确的估计结构的屈曲临界荷载,且应用简便,可供设计人员在工程设计中采用。

(2)本文提出的竖向均布荷载作用下临界荷载计算公式比Timoshenko提出的顶点集中荷载下临界荷载经典理论公式多了一个无量纲的系数 $\eta$ ,通过分析参数 $\rho$ 对参数 $\eta$ 的影响,给出可忽略参数 $\eta$ 时,参数 $\rho$ 的适用范围。

## 参考文献 References

- [1] 铁摩辛柯 S P. 弹性稳定理论[M]. 2版. 张福范,译. 北京:科学出版社,1965.  
TIMOSHENKO S P. Theory of elastic stability[M]. 2nd ed. ZHANG Fu-fan, translated. Beijing: Science press, 1965.
- [2] 李国强,刘玉姝,赵欣. 钢结构框架体系高等分析与系统可靠度设计[M]. 北京:中国建筑工业出版社,2006.  
LI Guo-qiang, LIU Yu-shu, ZHAO Xin. Higher analysis and reliability system design of the steel structure framework[M]. Beijing: China building industry press, 2006.
- [3] BAKKER M C M. Shear-flexural buckling of cantilever columns under uniformly distributed load [J]. Journal of engineering mechanics, 2006, 132(11):1160-1167.
- [4] 李亮,李国强,汪利. 水平荷载作用下新型钢-混凝土混合结构简化计算方法[J]. 建筑科学与工程学报, 2013, 30(4):1-8.  
LI Liang, LI Guo-qiang, WANG Li. Simplified Algorithm of the Multi-lateral Resistant Steel-concrete Mixed Structure under Lateral Load [J]. Journal of architecture and civil engineering, 2013, 30(4):1-8.
- [5] LI Liang, LI Guo-qiang, LUI Yu-shu. Simplified Algorithm of the Novel Steel-concrete Mixed Structure under Lateral Load [J]. International Journal of High-Rise Buildings, 2012, 1(4):247-254.
- [6] 童根树. 钢结构的平面内稳定[M]. 北京:中国建筑工业出版社,2005.  
TONG Gen-shu. The in-plane stability of steel structure[M]. Beijing: China building industry press, 2005.
- [7] 刘开国. 高层与大跨度结构简化分析技术及算例[M]. 北京:中国建筑工业出版社,2006.  
LIU Kai-guo. Simplify analysis and calculation examples of the tall and big span structure[M]. Beijing: China building industry press, 2006.
- [8] 李亮. 多重新型钢-混凝土混合结构设计方法及抗震性能研究[D]. 上海:同济大学,2011.  
LI Liang. Design approach and seismic behavior study on novel multi-lateral resistant steel-concrete mixed structure [D]. Shanghai: Tongji University, 2011.
- [9] 刘古岷,张若晞,张田申. 应用结构稳定计算[M]. 北京:科学出版社,2005.  
LIU Gu-min, ZHANG Nuo-xi, ZHANG Tian-shen. Stability computation of application structure[M]. Beijing: Science Press, 2005.

表2 参数 $\eta$ 与 $\rho$ 的相互关系

Tab. 2 Relation between the Parameter  $\eta$  and  $\rho$

编号	$\lambda$ 的范围	忽略 $\xi$ 引起的误差	编号	$\lambda$ 的范围	忽略 $\xi$ 引起的误差
1	<0.34或>17.36	<1%	6	<0.88或>6.61	<6%
2	<0.48或>12.09	<2%	7	<0.97或>6.03	<7%
3	<0.60或>9.63	<3%	8	<1.05或>5.57	<8%
4	<0.70或>8.37	<4%	9	<1.13或>5.15	<9%
5	<0.79或>7.35	<5%	10	<1.21或>4.8	<10%

(下转第828页)

- [7] 凌建明,林小平,赵鸿铎.圆柱形桥墩附近三维流场及河床局部冲刷分析[J].同济大学学报,2007(5):582-586.  
 LING Jian-ming, LIN Xiao-ping, ZHAO Hong-duo. Analysis of Three-Dimensional Flow Field and Local Scour of Riverbed Around Cylindrical Pier[J]. Journal of Tongji University, 2007(5):582-586.

## Bed fixed experimental study on velocity distribution of bridge piers with different intersection angles between bridge axle and flow direction

*YAN Jian-ke<sup>1,2</sup>, JIAO Chen<sup>1</sup>, LONG Tao<sup>1</sup>, YANG Jiu-cheng<sup>1</sup>, SHEN Bo<sup>2</sup>*

(1. Chinese First Institute Limited Corporation of Highway Survey & Design, Xi'an 710075, China;  
 2. Chang'an University, Xi'an 710064, China)

**Abstract:** By measuring the of velocity around multi-level bridge piers with different intersection angles between bridge axle and flow direction in fixed bed, the paper studies velocity distribution and hydrodynamic characteristics of bridge piers with different intersection angles between bridge axle and flow direction. The results show that bridge piers are arranged at different intersection angles between bridge axle and flow direction; that the piers influence each other, and that the piers in the upstream influence flow structure of the piers in the downstream. The disturbance can be attributed to three causes: near, shearing, and wake stream. When bridge piers are arranged at orthogonality between bridge axle and flow direction, velocity fluctuation in front of the piers or behind the pier is the biggest, but the affected region is the smallest. The smaller the intersection angle between bridge axle and flow direction bridge piers are arranged, the bigger velocity fluctuation in front of the piers or behind the pier, but the smaller the affected region.

**Key words:** *pier; intersection angle; velocity distribution; hydrodynamic characteristic; fixed bed*

---

**Biography:** YAN Jian-ke, Ph. D., Senior Engineer, Xi'an 710075, P. R. China, TEL: 0086-29-87906220-415, E-mail: yanjianke79@163.com

---

(上接第 821 页)

## Simplified algorithm of buckling critical load for shear-bending cantilever rod under axially uniformly distributed load

*LI Liang<sup>1</sup>, LI Guo-qiang<sup>2</sup>*

(1. College of Civil Engineering, Chang'an University, Xi'an 710061, China;  
 2. State Key Laboratory for Disaster Reduction in Civil Engineering, Tongji University, Shanghai 200092, China)

**Abstract:** According to the boundary conditions, bending and shear buckling displacement curves of vertical cantilever bar, the trigonometric function expressions are selected to approximately express the bending component and shear component of the vertical cantilever rod. Then the energy method is used to deduce the buckling critical load calculation formula of the shear bending cantilever bar under vertical uniform loads, and the reliability of the simplified algorithm is verified by compare with the results of finite element calculation. Finally, the result comparison between the recommended formulas under vertical uniformly distributed load in this paper and the Timoshenko equation under top-concentrated load are conducted, and one dimensionless coefficient are recognized. Then the accuracy of the formula is verified through the parameter analysis.

**Key words:** *vertical cantilever bar; boundary conditions; trigonometric function; bending component; buckling critical load*

---

**Biography:** LI Liang, Ph. D., Xi'an 710061, P. R. China, Tel: 0086-13991276215, E-mail: bright\_li@chd.edu.cn